

## Search for Lepton and Baryon Number Violating $\tau^-$ Decays into $\bar{p}\gamma$ , $\bar{p}\pi^0$ , $\bar{\Lambda}\pi^-$ , and $\Lambda\pi^-$

K. Abe,<sup>10</sup> K. Abe,<sup>46</sup> N. Abe,<sup>49</sup> I. Adachi,<sup>10</sup> H. Aihara,<sup>48</sup> M. Akatsu,<sup>24</sup> Y. Asano,<sup>53</sup>  
 T. Aso,<sup>52</sup> V. Aulchenko,<sup>2</sup> T. Aushev,<sup>14</sup> T. Aziz,<sup>44</sup> S. Bahinipati,<sup>6</sup> A. M. Bakich,<sup>43</sup>  
 Y. Ban,<sup>36</sup> M. Barbero,<sup>9</sup> A. Bay,<sup>20</sup> I. Bedny,<sup>2</sup> U. Bitenc,<sup>15</sup> I. Bizjak,<sup>15</sup> S. Blyth,<sup>29</sup>  
 A. Bondar,<sup>2</sup> A. Bozek,<sup>30</sup> M. Bračko,<sup>22,15</sup> J. Brodzicka,<sup>30</sup> T. E. Browder,<sup>9</sup> M.-C. Chang,<sup>29</sup>  
 P. Chang,<sup>29</sup> Y. Chao,<sup>29</sup> A. Chen,<sup>26</sup> K.-F. Chen,<sup>29</sup> W. T. Chen,<sup>26</sup> B. G. Cheon,<sup>4</sup>  
 R. Chistov,<sup>14</sup> S.-K. Choi,<sup>8</sup> Y. Choi,<sup>42</sup> Y. K. Choi,<sup>42</sup> A. Chuvikov,<sup>37</sup> S. Cole,<sup>43</sup>  
 M. Danilov,<sup>14</sup> M. Dash,<sup>55</sup> L. Y. Dong,<sup>12</sup> R. Dowd,<sup>23</sup> J. Dragic,<sup>23</sup> A. Drutskoy,<sup>6</sup>  
 S. Eidelman,<sup>2</sup> Y. Enari,<sup>24</sup> D. Epifanov,<sup>2</sup> C. W. Everton,<sup>23</sup> F. Fang,<sup>9</sup> S. Fratina,<sup>15</sup>  
 H. Fujii,<sup>10</sup> N. Gabyshev,<sup>2</sup> A. Garmash,<sup>37</sup> T. Gershon,<sup>10</sup> A. Go,<sup>26</sup> G. Gokhroo,<sup>44</sup>  
 B. Golob,<sup>21,15</sup> M. Grosse Perdekamp,<sup>38</sup> H. Guler,<sup>9</sup> J. Haba,<sup>10</sup> F. Handa,<sup>47</sup> K. Hara,<sup>10</sup>  
 T. Hara,<sup>34</sup> N. C. Hastings,<sup>10</sup> K. Hasuko,<sup>38</sup> K. Hayasaka,<sup>24</sup> H. Hayashii,<sup>25</sup> M. Hazumi,<sup>10</sup>  
 E. M. Heenan,<sup>23</sup> I. Higuchi,<sup>47</sup> T. Higuchi,<sup>10</sup> L. Hinz,<sup>20</sup> T. Hojo,<sup>34</sup> T. Hokuue,<sup>24</sup>  
 Y. Hoshi,<sup>46</sup> K. Hoshina,<sup>51</sup> S. Hou,<sup>26</sup> W.-S. Hou,<sup>29</sup> Y. B. Hsiung,<sup>29</sup> H.-C. Huang,<sup>29</sup>  
 T. Igaki,<sup>24</sup> Y. Igarashi,<sup>10</sup> T. Iijima,<sup>24</sup> A. Imoto,<sup>25</sup> K. Inami,<sup>24</sup> A. Ishikawa,<sup>10</sup> H. Ishino,<sup>49</sup>  
 K. Itoh,<sup>48</sup> R. Itoh,<sup>10</sup> M. Iwamoto,<sup>3</sup> M. Iwasaki,<sup>48</sup> Y. Iwasaki,<sup>10</sup> R. Kagan,<sup>14</sup> H. Kakuno,<sup>48</sup>  
 J. H. Kang,<sup>56</sup> J. S. Kang,<sup>17</sup> P. Kapusta,<sup>30</sup> S. U. Kataoka,<sup>25</sup> N. Katayama,<sup>10</sup> H. Kawai,<sup>3</sup>  
 H. Kawai,<sup>48</sup> Y. Kawakami,<sup>24</sup> N. Kawamura,<sup>1</sup> T. Kawasaki,<sup>32</sup> N. Kent,<sup>9</sup> H. R. Khan,<sup>49</sup>  
 A. Kibayashi,<sup>49</sup> H. Kichimi,<sup>10</sup> H. J. Kim,<sup>19</sup> H. O. Kim,<sup>42</sup> Hyunwoo Kim,<sup>17</sup> J. H. Kim,<sup>42</sup>  
 S. K. Kim,<sup>41</sup> T. H. Kim,<sup>56</sup> K. Kinoshita,<sup>6</sup> P. Koppenburg,<sup>10</sup> S. Korpar,<sup>22,15</sup> P. Križan,<sup>21,15</sup>  
 P. Krokovny,<sup>2</sup> R. Kulasiri,<sup>6</sup> C. C. Kuo,<sup>26</sup> H. Kurashiro,<sup>49</sup> E. Kurihara,<sup>3</sup> A. Kusaka,<sup>48</sup>  
 A. Kuzmin,<sup>2</sup> Y.-J. Kwon,<sup>56</sup> J. S. Lange,<sup>7</sup> G. Leder,<sup>13</sup> S. E. Lee,<sup>41</sup> S. H. Lee,<sup>41</sup> Y.-J. Lee,<sup>29</sup>  
 T. Lesiak,<sup>30</sup> J. Li,<sup>40</sup> A. Limosani,<sup>23</sup> S.-W. Lin,<sup>29</sup> D. Liventsev,<sup>14</sup> J. MacNaughton,<sup>13</sup>  
 G. Majumder,<sup>44</sup> F. Mandl,<sup>13</sup> D. Marlow,<sup>37</sup> T. Matsuishi,<sup>24</sup> H. Matsumoto,<sup>32</sup>  
 S. Matsumoto,<sup>5</sup> T. Matsumoto,<sup>50</sup> A. Matyja,<sup>30</sup> Y. Mikami,<sup>47</sup> W. Mitaroff,<sup>13</sup>  
 K. Miyabayashi,<sup>25</sup> Y. Miyabayashi,<sup>24</sup> Y. Miyazaki,<sup>24</sup> H. Miyake,<sup>34</sup> H. Miyata,<sup>32</sup> R. Mizuk,<sup>14</sup>  
 D. Mohapatra,<sup>55</sup> G. R. Moloney,<sup>23</sup> G. F. Moorhead,<sup>23</sup> T. Mori,<sup>49</sup> A. Murakami,<sup>39</sup>  
 T. Nagamine,<sup>47</sup> Y. Nagasaka,<sup>11</sup> T. Nakadaira,<sup>48</sup> I. Nakamura,<sup>10</sup> E. Nakano,<sup>33</sup> M. Nakao,<sup>10</sup>  
 H. Nakazawa,<sup>10</sup> Z. Natkaniec,<sup>30</sup> K. Neichi,<sup>46</sup> S. Nishida,<sup>10</sup> O. Nitoh,<sup>51</sup> S. Noguchi,<sup>25</sup>  
 T. Nozaki,<sup>10</sup> A. Ogawa,<sup>38</sup> S. Ogawa,<sup>45</sup> T. Ohshima,<sup>24</sup> T. Okabe,<sup>24</sup> S. Okuno,<sup>16</sup>  
 S. L. Olsen,<sup>9</sup> Y. Onuki,<sup>32</sup> W. Ostrowicz,<sup>30</sup> H. Ozaki,<sup>10</sup> P. Pakhlov,<sup>14</sup> H. Palka,<sup>30</sup>  
 C. W. Park,<sup>42</sup> H. Park,<sup>19</sup> K. S. Park,<sup>42</sup> N. Parslow,<sup>43</sup> L. S. Peak,<sup>43</sup> M. Pernicka,<sup>13</sup>  
 J.-P. Perroud,<sup>20</sup> M. Peters,<sup>9</sup> L. E. Piilonen,<sup>55</sup> A. Poluektov,<sup>2</sup> F. J. Ronga,<sup>10</sup> N. Root,<sup>2</sup>

M. Rozanska,<sup>30</sup> H. Sagawa,<sup>10</sup> M. Saigo,<sup>47</sup> S. Saitoh,<sup>10</sup> Y. Sakai,<sup>10</sup> H. Sakamoto,<sup>18</sup>  
T. R. Sarangi,<sup>10</sup> M. Satapathy,<sup>54</sup> N. Sato,<sup>24</sup> O. Schneider,<sup>20</sup> J. Schümann,<sup>29</sup> C. Schwanda,<sup>13</sup>  
A. J. Schwartz,<sup>6</sup> T. Seki,<sup>50</sup> S. Semenov,<sup>14</sup> K. Senyo,<sup>24</sup> Y. Settai,<sup>5</sup> R. Seuster,<sup>9</sup>  
M. E. Sevier,<sup>23</sup> T. Shibata,<sup>32</sup> H. Shibuya,<sup>45</sup> B. Shwartz,<sup>2</sup> V. Sidorov,<sup>2</sup> V. Siegle,<sup>38</sup>  
J. B. Singh,<sup>35</sup> A. Somov,<sup>6</sup> N. Soni,<sup>35</sup> R. Stamen,<sup>10</sup> S. Stanič,<sup>53,\*</sup> M. Starič,<sup>15</sup> A. Sugi,<sup>24</sup>  
A. Sugiyama,<sup>39</sup> K. Sumisawa,<sup>34</sup> T. Sumiyoshi,<sup>50</sup> S. Suzuki,<sup>39</sup> S. Y. Suzuki,<sup>10</sup> O. Tajima,<sup>10</sup>  
F. Takasaki,<sup>10</sup> K. Tamai,<sup>10</sup> N. Tamura,<sup>32</sup> K. Tanabe,<sup>48</sup> M. Tanaka,<sup>10</sup> G. N. Taylor,<sup>23</sup>  
Y. Teramoto,<sup>33</sup> X. C. Tian,<sup>36</sup> S. Tokuda,<sup>24</sup> S. N. Tovey,<sup>23</sup> K. Trabelsi,<sup>9</sup> T. Tsuboyama,<sup>10</sup>  
T. Tsukamoto,<sup>10</sup> K. Uchida,<sup>9</sup> S. Uehara,<sup>10</sup> T. Uglov,<sup>14</sup> K. Ueno,<sup>29</sup> Y. Unno,<sup>3</sup> S. Uno,<sup>10</sup>  
Y. Ushiroda,<sup>10</sup> G. Varner,<sup>9</sup> K. E. Varvell,<sup>43</sup> S. Villa,<sup>20</sup> C. C. Wang,<sup>29</sup> C. H. Wang,<sup>28</sup>  
J. G. Wang,<sup>55</sup> M.-Z. Wang,<sup>29</sup> M. Watanabe,<sup>32</sup> Y. Watanabe,<sup>49</sup> L. Widhalm,<sup>13</sup>  
Q. L. Xie,<sup>12</sup> B. D. Yabsley,<sup>55</sup> A. Yamaguchi,<sup>47</sup> H. Yamamoto,<sup>47</sup> S. Yamamoto,<sup>50</sup>  
T. Yamanaka,<sup>34</sup> Y. Yamashita,<sup>31</sup> M. Yamauchi,<sup>10</sup> Heyoung Yang,<sup>41</sup> P. Yeh,<sup>29</sup> J. Ying,<sup>36</sup>  
K. Yoshida,<sup>24</sup> Y. Yuan,<sup>12</sup> Y. Yusa,<sup>47</sup> H. Yuta,<sup>1</sup> S. L. Zang,<sup>12</sup> C. C. Zhang,<sup>12</sup> J. Zhang,<sup>10</sup>  
L. M. Zhang,<sup>40</sup> Z. P. Zhang,<sup>40</sup> V. Zhilich,<sup>2</sup> T. Ziegler,<sup>37</sup> D. Žontar,<sup>21,15</sup> and D. Zürcher<sup>20</sup>

(The Belle Collaboration)

<sup>1</sup>*Aomori University, Aomori*

<sup>2</sup>*Budker Institute of Nuclear Physics, Novosibirsk*

<sup>3</sup>*Chiba University, Chiba*

<sup>4</sup>*Chonnam National University, Kwangju*

<sup>5</sup>*Chuo University, Tokyo*

<sup>6</sup>*University of Cincinnati, Cincinnati, Ohio 45221*

<sup>7</sup>*University of Frankfurt, Frankfurt*

<sup>8</sup>*Gyeongsang National University, Chinju*

<sup>9</sup>*University of Hawaii, Honolulu, Hawaii 96822*

<sup>10</sup>*High Energy Accelerator Research Organization (KEK), Tsukuba*

<sup>11</sup>*Hiroshima Institute of Technology, Hiroshima*

<sup>12</sup>*Institute of High Energy Physics,*

*Chinese Academy of Sciences, Beijing*

<sup>13</sup>*Institute of High Energy Physics, Vienna*

<sup>14</sup>*Institute for Theoretical and Experimental Physics, Moscow*

<sup>15</sup>*J. Stefan Institute, Ljubljana*

<sup>16</sup>*Kanagawa University, Yokohama*

<sup>17</sup>*Korea University, Seoul*

<sup>18</sup>*Kyoto University, Kyoto*

<sup>19</sup>*Kyungpook National University, Taegu*

<sup>20</sup>*Swiss Federal Institute of Technology of Lausanne, EPFL, Lausanne*

<sup>21</sup>*University of Ljubljana, Ljubljana*

- <sup>22</sup>University of Maribor, Maribor
- <sup>23</sup>University of Melbourne, Victoria
- <sup>24</sup>Nagoya University, Nagoya
- <sup>25</sup>Nara Women's University, Nara
- <sup>26</sup>National Central University, Chung-li
- <sup>27</sup>National Kaohsiung Normal University, Kaohsiung
- <sup>28</sup>National United University, Miao Li
- <sup>29</sup>Department of Physics, National Taiwan University, Taipei
- <sup>30</sup>H. Niewodniczanski Institute of Nuclear Physics, Krakow
- <sup>31</sup>Nihon Dental College, Niigata
- <sup>32</sup>Niigata University, Niigata
- <sup>33</sup>Osaka City University, Osaka
- <sup>34</sup>Osaka University, Osaka
- <sup>35</sup>Panjab University, Chandigarh
- <sup>36</sup>Peking University, Beijing
- <sup>37</sup>Princeton University, Princeton, New Jersey 08545
- <sup>38</sup>RIKEN BNL Research Center, Upton, New York 11973
- <sup>39</sup>Saga University, Saga
- <sup>40</sup>University of Science and Technology of China, Hefei
- <sup>41</sup>Seoul National University, Seoul
- <sup>42</sup>Sungkyunkwan University, Suwon
- <sup>43</sup>University of Sydney, Sydney NSW
- <sup>44</sup>Tata Institute of Fundamental Research, Bombay
- <sup>45</sup>Toho University, Funabashi
- <sup>46</sup>Tohoku Gakuin University, Tagajo
- <sup>47</sup>Tohoku University, Sendai
- <sup>48</sup>Department of Physics, University of Tokyo, Tokyo
- <sup>49</sup>Tokyo Institute of Technology, Tokyo
- <sup>50</sup>Tokyo Metropolitan University, Tokyo
- <sup>51</sup>Tokyo University of Agriculture and Technology, Tokyo
- <sup>52</sup>Toyama National College of Maritime Technology, Toyama
- <sup>53</sup>University of Tsukuba, Tsukuba
- <sup>54</sup>Utkal University, Bhubaneswer
- <sup>55</sup>Virginia Polytechnic Institute and State University, Blacksburg, Virginia 24061
- <sup>56</sup>Yonsei University, Seoul

## Abstract

We have searched for decays that violate both lepton and baryon number using data collected by the Belle detector at the KEKB asymmetric  $e^+e^-$  collider. No signals are found in  $\tau^- \rightarrow \bar{p}\gamma$ ,  $\tau^- \rightarrow \bar{p}\pi^0$ ,  $\tau^- \rightarrow \bar{\Lambda}\pi^-$ , and  $\tau^- \rightarrow \Lambda\pi^-$  and we set upper limits on the branching fractions of  $\mathcal{B}(\tau^- \rightarrow \bar{p}\gamma) < 3.0 \times 10^{-7}$ ,  $\mathcal{B}(\tau^- \rightarrow \bar{p}\pi^0) < 6.5 \times 10^{-7}$ ,  $\mathcal{B}(\tau^- \rightarrow \bar{\Lambda}\pi^-) < 1.3 \times 10^{-7}$ , and  $\mathcal{B}(\tau^- \rightarrow \Lambda\pi^-) < 0.70 \times 10^{-7}$  at the 90% confidence level. The former two results improve the previous limits by a factor of 12 and 23, respectively, while the latter two are the first searches ever performed.

PACS numbers: 11.30.-j, 12.60.-i, 13.35.Dx, 14.60.Fg

## INTRODUCTION

While the Standard Model (SM) assumes both the baryon number ( $B$ ) and lepton number ( $L$ ) conservation, in some extensions beyond the SM such as Grand Unified Theories (GUTs),  $B$  and  $L$  violation is expected while their difference  $B - L$  is conserved [1]. In Ref. [2], right-handed four-fermion couplings that conserve  $B - L$  were used to consider  $B$  and  $L$  violating  $\tau$  lepton,  $D$  and  $B$  meson decays. High luminosity B-factories provide an opportunity to look for such decays with unprecedented sensitivity.

We report here our searches for  $\tau^- \rightarrow \bar{p}\gamma$ ,  $\bar{p}\pi^0$ ,  $\bar{\Lambda}\pi^-$ , and  $\Lambda\pi^-$  decays with data samples of  $86.7 \text{ fb}^{-1}$  for  $\bar{p}\gamma$  and  $153.8 \text{ fb}^{-1}$  for all other modes, collected with the Belle detector at the KEKB asymmetric  $e^+e^-$  collider [3]. Previously, the best upper limits for the corresponding branching fractions were obtained by CLEO [4] based on a data sample of  $4.7 \text{ fb}^{-1}$ :  $\mathcal{B}(\tau^- \rightarrow \bar{p}\gamma) < 3.5 \times 10^{-6}$  and  $\mathcal{B}(\tau^- \rightarrow \bar{p}\pi^0) < 1.5 \times 10^{-5}$  at 90% C.L. The decay modes  $\tau^- \rightarrow \bar{\Lambda}\pi^-$  and  $\tau^- \rightarrow \Lambda\pi^-$  have never been studied before. Unless otherwise stated, charge conjugate decays are implied throughout this paper.

The Belle detector is a large-solid-angle magnetic spectrometer that consists of a silicon vertex detector (SVD), a 50-layer central drift chamber (CDC), an array of aerogel threshold Čerenkov counters (ACC), a barrel-like arrangement of time-of-flight scintillation counters (TOF), and an electromagnetic calorimeter comprised of CsI(Tl) crystals (ECL) located inside a superconducting solenoid coil that provides a 1.5 T magnetic field. An iron flux-return located outside of the coil is instrumented to detect  $K_L^0$  mesons and to identify muons (KLM). The detector is described in detail elsewhere [5].

We search for  $\tau^+\tau^-$  events in which one  $\tau$  decays into the mode studied (signal side) and the other  $\tau$  (tag side) decays into one charged particle, photons and neutrino(s). The selection criteria are determined by examining Monte Carlo (MC) simulations for signal  $\tau$ -pair decays and background (BG) events coming from generic  $\tau$ -pair decays ( $\tau^+\tau^-$ ),  $q\bar{q}$  continuum,  $B\bar{B}$ , Bhabha and  $\mu\mu$  as well as two-photon processes. The KORALB/TAUOLA [6] and QQ [7] generators are used for event generation, and GEANT3 [8] is used to simulate the Belle detector response. The two-body decays of the signal  $\tau$  are assumed to have a uniform angular distribution in the  $\tau$ 's rest frame. All the kinematical variables are calculated in the laboratory frame, while those in the  $e^+e^-$  center-of-mass (CM) frame are indicated by the superscript "CM".

## ANALYSIS OF $\tau^- \rightarrow \bar{p}\gamma$ AND $\bar{p}\pi^0$

### Event selection

The experimental signature of these events has one  $\tau$  lepton decaying into a proton and photons (signal side) and the other decaying via the 1-prong mode (tag side):

$$\left\{ \tau^- \rightarrow \bar{p} + n_\gamma^{\text{SIG}} \right\} + \left\{ \tau^+ \rightarrow (\text{a track})^+ + n_\gamma^{\text{TAG}} + X(\text{missing}) \right\}, \quad (1)$$

where a track should have transverse momentum  $p_t > 0.1$  GeV/ $c$  and polar angle  $-0.819 < \cos\theta < 0.906$ . The two highlighted tracks should have zero net charge. A proton track forming the signal  $\bar{p}\gamma/\bar{p}\pi^0$  is required to have  $p > 1.0$  GeV/ $c$  for reliable identification. A photon should have energy  $E_\gamma > 0.1$  GeV in the same polar angle range as that for tracks. The number of photons on the signal side is  $1 < (n_\gamma^{\text{SIG}} + n_\gamma^{\text{TAG}}) < 3$  for  $\tau^- \rightarrow \bar{p}\gamma$  and  $2 < (n_\gamma^{\text{SIG}} + n_\gamma^{\text{TAG}}) < 4$  for  $\tau^- \rightarrow \bar{p}\pi^0$ .

We divide the event into two hemispheres in the CM frame by the plane perpendicular to the thrust axis. The hemisphere containing a proton track (its identification is later explained), is the 'signal side', the opposite hemisphere is the 'tag side'. We require an invariant mass of the visible particles on the tag side of  $M_{\text{TAG}} < 1.2$  GeV/ $c^2$  for the  $\bar{p}\gamma$  mode and  $M_{\text{TAG}} < m_\tau$  for the  $\bar{p}\pi^0$  one to reduce background (BG) from the  $e^+e^- \rightarrow q\bar{q}$  continuum process (where  $q = u, d, s, c$ ).

For  $\bar{p}\gamma$ , we require the photon to have  $E_\gamma > 0.5$  GeV. In order to reduce the number of fake  $\gamma$ 's originating from a  $\bar{n}$  in the  $q\bar{q}$  continuum, the ratio of photon energy deposition in a  $3 \times 3$  ECL square to a  $5 \times 5$  square,  $E9/E25$ , is required to be larger than 0.93 since the hadronic shower of a  $\bar{n}$  in the ECL is wider than a photon's electromagnetic shower.

The  $\pi^0$  from  $\bar{p}\pi^0$  is reconstructed from a  $\gamma\gamma$  pair with an invariant mass within  $\pm 5\sigma_{\pi^0}$  ( $\sigma_{\pi^0} = 5 - 8$  MeV/ $c^2$ ) of the nominal  $\pi^0$  mass. We impose a  $\pi^0$  veto on photon(s) for  $\bar{p}\gamma/\bar{p}\pi^0$  candidates: it should not reconstruct a  $\pi^0$  meson when combined with any other photon whose energy exceeds 50 MeV.

Correlations are considered among the tracks, photons and a missing particle that carries away undetected momentum and energy. A requirement on the total visible energy  $0.5 < E_{\text{vis}}^{\text{CM}}/\sqrt{s} < 0.92$  is imposed to reject Bhabha scattering and  $\mu^+\mu^-$  production. Restrictions on the opening angle between  $p$  and  $\gamma$ , and  $p$  and  $\pi^0$  reduce BG from the generic  $\tau^+\tau^-$  and  $q\bar{q}$  continuum:  $0.6 < \cos\theta_{p\gamma}^{\text{CM}} < 0.96$  and  $0.0 < \cos\theta_{p\pi^0}^{\text{CM}} < 0.95$ . The opening angle between the two tracks in the CM frame is also required to be larger than  $90^\circ$ . Constraints on the missing momentum  $p_{\text{miss}}$  and polar-angle  $\theta_{\text{miss}}$  are imposed to ensure that the missing particles are undetected neutrino(s) rather than photons or charged particles that escaped detection:  $p_{\text{miss}} > 0.6$  GeV/ $c$  for  $\bar{p}\gamma$  and  $p_{\text{miss}} > 0.5$  GeV/ $c$  for  $\bar{p}\pi^0$ , and  $-0.866 < \cos\theta_{\text{miss}} < 0.956$  for both modes. A requirement on the opening angle  $\theta_{\text{tag-miss}}^{\text{CM}}$  between the tag-side track and the missing particle helps to remove  $\tau^+\tau^-$  events:  $\cos\theta_{\text{tag-miss}}^{\text{CM}} > 0.3$  for  $\bar{p}\gamma$  and  $\cos\theta_{\text{tag-miss}}^{\text{CM}} > 0.0$  for  $\bar{p}\pi^0$ .

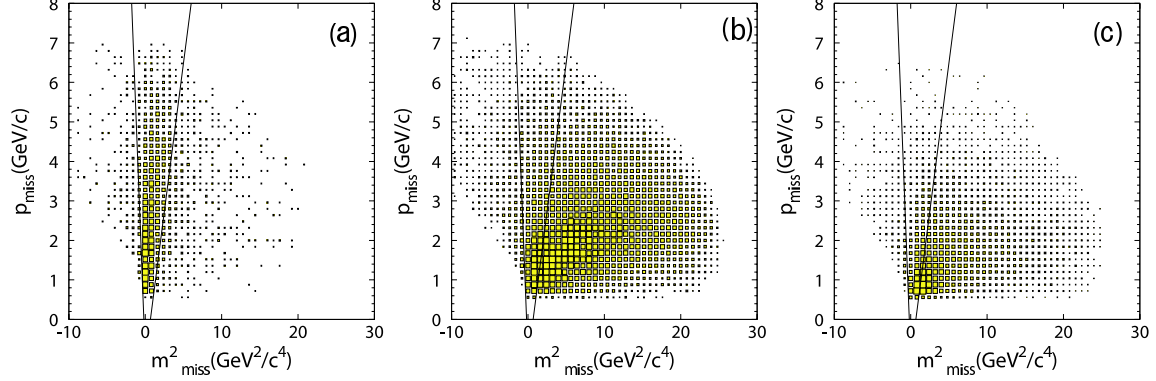


FIG. 1:  $p_{\text{miss}}$  vs  $m_{\text{miss}}^2$  plots of  $\tau^- \rightarrow \bar{p}\gamma$ : (a) signal MC, (b)  $\tau^+\tau^-$  MC and (c)  $q\bar{q}$  ( $uds$ ) continuum MC. The area between the lines is the selected region.

An additional condition is imposed on the relation between  $p_{\text{miss}}$  and the mass squared of a missing particle  $m_{\text{miss}}^2$  (see Fig.1):  $p_{\text{miss}} > -3 m_{\text{miss}}^2 - 1$  and  $p_{\text{miss}} > 1.2 m_{\text{miss}}^2 - 1$  for  $\bar{p}\gamma$ , and  $p_{\text{miss}} > -0.8 m_{\text{miss}}^2 + 0.3$  and  $p_{\text{miss}} > 1.6 m_{\text{miss}}^2 - 1$  for  $\bar{p}\pi^0$ . This cut removes 81% of the remaining  $\tau^+\tau^-$  and 73% of continuum BG's while retaining 78% of the signal.

Particle identification, that is very important in this measurement, is based on the responses of subdetectors such as the ratio of the energy deposited in ECL to the momentum measured by CDC, the shower shape in ECL, particle range in KLM, the hit information from the threshold type ACC,  $dE/dX$  in CDC and time-of-flight from TOF. We use likelihood ratios to distinguish hadron species, for instance,  $\mathcal{P}(p/\pi) = \mathcal{L}_p/(\mathcal{L}_p + \mathcal{L}_\pi)$ , where  $\mathcal{L}_i$  is the likelihood for the detector response to the track with flavor hypothesis  $i$ . For lepton identification, we use an electron probability  $\mathcal{P}(e)$  and a muon probability  $\mathcal{P}(\mu)$  determined by the detector responses.

We demand  $\mathcal{P}(e) < 0.8$  and  $\mathcal{P}(\mu) < 0.8$  for the signal-side track in order to remove Bhabha and  $\mu^+\mu^-$  processes. To identify protons, the ACC plays an important role since it allows us to distinguish flavors by the threshold momentum: for protons, this is  $p_{\text{p-th}}^{\text{ACC}} \simeq 5$  GeV/ $c$  in the barrel region and  $\simeq 4$  GeV/ $c$  in the forward endcap, while for pions is  $p_{\pi\text{-th}}^{\text{ACC}} > 1$  GeV/ $c$ .

Most BG tracks are pions with a rather high momentum up to 5 GeV/ $c$ , and the momentum of most protons ranges from 1 to 5 GeV/ $c$ . Therefore, we can identify protons and remove pions by requiring ACC not to fire at  $1 \text{ GeV}/c < p < p_{\text{p-th}}^{\text{ACC}}$ . With these criteria, 90% of the BG is removed, while 80% of the signal remains.

The information from TOF and CDC is combined with that from the ACC into  $\mathcal{L}_p$  and  $\mathcal{L}_\pi$  to further reduce  $\pi$  BG as well as  $K$ 's in  $\bar{p}\pi^0$ . The requirement  $\mathcal{P}(p/\pi) > 0.8$  removes more than 90% of the BG while retaining 87% of the signal. In the  $\bar{p}\pi^0$  mode, background processes with kaons, mostly from  $\tau \rightarrow K^*\nu$  and  $K^* \rightarrow K\pi^0$  are rejected by demanding  $\mathcal{P}(p/K) > 0.8$ : 70% of the  $K$ 's are removed while 77% of the signal is retained.



## Expected backgrounds and blind analysis

A signal candidate is examined in the two-dimensional space of the  $\bar{p}\gamma/\bar{p}\pi^0$  invariant mass,  $M_{\text{inv}}$ , and the difference of its energy from the beam energy in the CM system,  $\Delta E$ . A signal event should have  $M_{\text{inv}} \simeq m_\tau$  and  $\Delta E \simeq 0$ . The  $M_{\text{inv}}$  and  $\Delta E$  resolutions are evaluated from the MC distributions around the peak using an asymmetric Gaussian shape to account for initial state radiation and ECL energy leakage for photons:  $\sigma_{M_{\text{inv}}}^{\text{high/low}} = 10.7/16.7$  MeV/ $c^2$  and  $\sigma_{\Delta E}^{\text{high/low}} = 35.2/62.8$  MeV for the  $\bar{p}\gamma$ , and  $\sigma_{M_{\text{inv}}}^{\text{high/low}} = 11.3/14.9$  MeV/ $c^2$  and  $\sigma_{\Delta E}^{\text{high/low}} = 34.3/57.1$  MeV for the  $\bar{p}\pi^0$ , where the ‘‘high/low’’ superscript indicates the higher/lower side of the peak.

To avoid any bias in extracting the result, we blind the following region:  $\pm 5\sigma_{M_{\text{inv}}}$  and  $\pm 5\sigma_{\Delta E}$  for  $\bar{p}\gamma$ , and the  $1.68 \text{ GeV}/c^2 < M_{\text{inv}} < 1.85 \text{ GeV}/c^2$  band region for  $\bar{p}\pi^0$  (see Fig. 2). Since the  $\pm 5\sigma$  region for the  $\bar{p}\pi^0$  mode contains significantly more events than in the  $\bar{p}\gamma$  case, we blind a wider region for the former mode.

To estimate the expected number of BG events in the blinded region, we approximate the data distribution by a combination of Landau and Gaussian functions with a few parameters in the region  $1.42 \text{ GeV}/c^2 < M_{\text{inv}} < 2.10 \text{ GeV}/c^2$  for  $\bar{p}\gamma$ , and by an asymmetric Gaussian function with a few parameters in the region  $1.5 \text{ GeV}/c^2 < M_{\text{inv}} < 2.0 \text{ GeV}/c^2$  for  $\bar{p}\pi^0$  as shown in Fig. 3. One finds in these areas, excluding the blinded region, 49 and 195 data events for  $\bar{p}\gamma$  and  $\bar{p}\pi^0$ , respectively, and  $51.8 \pm 6.1$  and  $178.4 \pm 12.8$  corresponding MC events (properly normalized to the luminosity of the data), after application of all cuts. The number of BG events expected from the BG functions in the  $5\sigma$  regions is  $9.1 \pm 1.7$  and  $52.2 \pm 7.3$  events for  $\bar{p}\gamma$  and  $\bar{p}\pi^0$ , respectively. The independent evaluation of the number of BG events in the  $5\sigma$  regions based on the MC simulation of the BG processes gave  $6.1 \pm 2.0$  and  $43.4 \pm 6.6$  events for  $\bar{p}\gamma$  and  $\bar{p}\pi^0$ , respectively, in reasonable agreement with the sideband based evaluation above. The data and signal MC distributions in  $\Delta E$  vs  $M_{\text{inv}}$  are shown for both modes in Fig. 2.

The signal detection efficiency for the  $\pm 5\sigma$  box is evaluated from MC as 9.4% and 5.8% for  $\bar{p}\gamma$  and  $\bar{p}\pi^0$ , respectively.

## Blind opening and evaluation of the branching fractions

Data distributions after opening the blinded regions are shown in Figs. 2 and 3. We find 16 and 70 events in the  $5\sigma$  regions for  $\bar{p}\gamma$  and  $\bar{p}\pi^0$ , respectively, while the number of expected BG events is  $9.1 \pm 1.7$  and  $52.2 \pm 7.3$  as evaluated above using the data sidebands. The differences between the number of observed data events and the BG expectations,  $6.9 \pm 4.3$  for  $\bar{p}\gamma$  and  $17.8 \pm 11.1$  for  $\bar{p}\pi^0$ , are not statistically significant.

To extract the number of signal events, we applied an unbinned extended maximum likelihood method (UEML), which is more sensitive than the binned one since it uses the



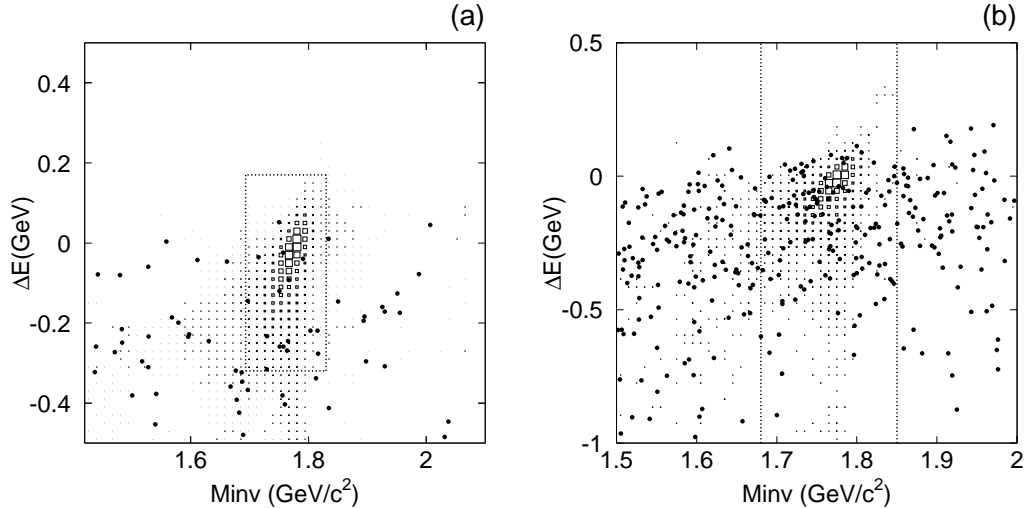


FIG. 2:  $\Delta E - M_{\text{inv}}$  plot after opening the blind areas (inside the dotted lines) for (a)  $\bar{p}\gamma$  and (b)  $\bar{p}\pi^0$  decay modes. The data are shown by bold dots and the signal MC by the boxes.

complete information about events. In this method the likelihood function is defined as

$$\mathcal{L}(s, b) = \frac{e^{-(s+b)}}{N!} \prod_{i=1}^N (sS_i + bB_i), \quad (2)$$

where  $N$  is the number of the observed events,  $s$  and  $b$  are the free parameters corresponding to the number of signal and background events, respectively, and  $S_i$  and  $B_i$  are the values of the probability density functions of the signal and BG for the  $i$ -th event.  $S_i$  is given by the signal MC distributions, and  $B_i$  is the BG function obtained above and normalized to unity.

The maximum likelihood fit for the  $\pm 5\sigma$  region yields  $s_0 = 0.16$  and  $b_0 = 15.84$  for  $\bar{p}\gamma$  and  $s_0 = 3.09$  and  $b_0 = 66.91$  for  $\bar{p}\pi^0$ , respectively. Following Ref. [9], the upper limit at the 90% confidence level (C.L.) is obtained by means of toy MC, as described below. For every assumed expected signal yield  $\tilde{s}$ , 10,000 samples are generated, for each of which the number of signal and BG events is determined by Poisson statistics with the mean values  $\tilde{s}$  and  $b_0$ , respectively. We then assign the  $\Delta E$  and  $M_{\text{inv}}$  values to these events according to their distributions; a UEML fit is performed for every prepared sample to extract the signal yield ( $\tilde{s}_0$ ); the confidence level for an assumed  $\tilde{s}$  is defined as the fraction of the samples whose  $\tilde{s}_0$  exceeds  $\tilde{s}$ . This procedure is repeated until we find the value of  $\tilde{s}_{90}$  that gives a 90% chance of  $\tilde{s}_0$  being larger than  $\tilde{s}$ . The resulting values are  $\tilde{s}_{90} = 3.7$  events for  $\bar{p}\gamma$  and  $\tilde{s}_{90} = 9.8$  events for  $\bar{p}\pi^0$ .

The upper limit on the branching fraction  $\mathcal{B}$  at the 90% C.L. is then calculated as

$$\mathcal{B} < \frac{\tilde{s}_{90}}{2\varepsilon N_{\tau\tau}}, \quad (3)$$

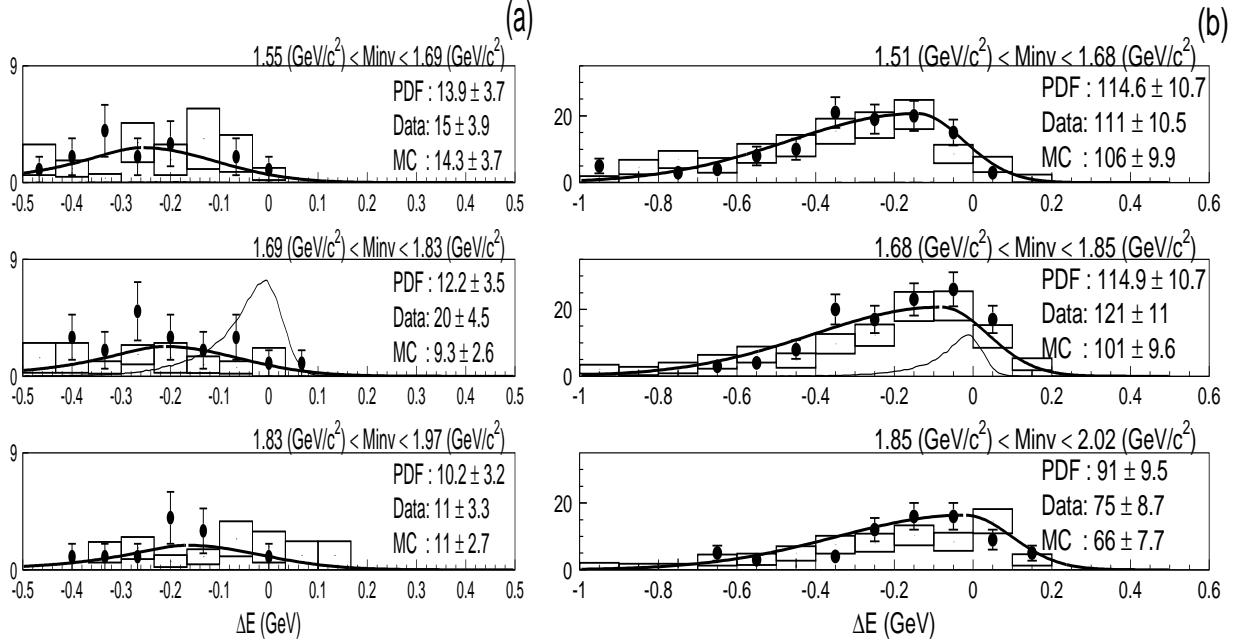


FIG. 3: The  $\Delta E$  distributions for (a)  $\bar{p}\gamma$  and (b)  $\bar{p}\pi^0$ . In both (a) and (b) the upper, middle and lower figures correspond to the indicated  $M_{\text{inv}}$  regions: the middle one is the blind area while the upper and lower correspond to the sidebands. All three regions have the same width. The closed circles with error bars are the data observed after opening the signal box, the histogram with error rectangles shows the results of MC simulation for the BG processes (generic  $\tau^+\tau^-$  and continuum  $q\bar{q}$ ). The thick solid curve shows the contribution of the BG parameterized in the sideband regions. The expected signal ( $\mathcal{B} = 10 \times 10^{-7}$ ) is shown by the thin solid line. The data in the middle figures are blinded until the last stage of the analysis.

where the number of produced  $\tau$ -pairs is  $N_{\tau\tau} = 78.9 \times 10^6$  and  $140.0 \times 10^6$  for  $\bar{p}\gamma$  and  $\bar{p}\pi^0$ , respectively, and the detection efficiencies are  $\varepsilon = 9.4\%$  and  $5.8\%$ . The resulting upper limits are  $\mathcal{B}(\tau^- \rightarrow \bar{p}\gamma) < 2.5 \times 10^{-7}$  and  $\mathcal{B}(\tau^- \rightarrow \bar{p}\pi^0) < 6.1 \times 10^{-7}$  at 90% C.L.

Systematic uncertainties related to the detector sensitivity  $2\varepsilon N_{\tau\tau}$  in the denominator of Eq. (3) are evaluated to be 5.9% for  $\bar{p}\gamma$  and 8.7% for  $\bar{p}\pi^0$ . The individual contributions to the uncertainties for  $\bar{p}\gamma$  ( $\bar{p}\pi^0$ ) are 2.0%(2.0%) from tracking efficiency, 3.0%(6.0%) from photon reconstruction efficiency, 2.0%(4.0%) from selection criteria, 3.0%(3.0%) from trigger efficiency, 2.5%(3.0%) from proton identification, 0.2%(0.3%) from MC statistics, 1.4%(1.4%) from luminosity evaluation, and 0.03%(0.03%) from the  $\tau^+\tau^-$  cross-section.

The systematic uncertainty in  $\tilde{s}_{90}$  is estimated by varying the parameters of the BG functions by  $\pm 1\sigma$ . This gives uncertainties of  $\pm 0.77$  events for  $\bar{p}\gamma$  and  $\pm 0.75$  events for  $\bar{p}\pi^0$ . The upper limits on the branching fractions taking into account all the systematic uncertainties are calculated to be

$$\mathcal{B}(\tau^- \rightarrow \bar{p}\gamma) < 3.0 \times 10^{-7} \quad (4)$$

$$\mathcal{B}(\tau^- \rightarrow \bar{p}\pi^0) < 6.5 \times 10^{-7} \quad (5)$$

at 90% C.L. with  $86.7 \text{ fb}^{-1}$  and  $153.8 \text{ fb}^{-1}$  of data, respectively.

The  $\bar{p}\pi^0$  mode should be discussed briefly since some excess of events in the signal area can be seen in the  $\Delta E$  distribution of Fig. 3. From the  $s$  dependence of the likelihood function, a 68% confidence interval for  $s_0$  is  $-1.6 < s_0 < 8.8$ ; in other words,  $s_0$  is consistent with 0 within  $1 \sigma$ . If we use toy MC, a probability to have  $s_0 > 3.09$  when the signal yield  $\tilde{s} = 0$  is 19%. We conclude that the observed excess can be due a statistical fluctuation.

## ANALYSIS OF $\tau^- \rightarrow \bar{\Lambda}\pi^-$ AND $\Lambda\pi^-$

### Event Selection

The experimental signature of these events has one  $\tau$  lepton (signal side) decaying to  $\Lambda\pi$ ,  $\Lambda$  to  $p\pi$  and the other (tag side) decaying via a 1-prong mode:

$$\{\tau^- \rightarrow (\bar{p}\pi^+) + \pi^-\} + \{\tau^+ \rightarrow (\text{a track})^+ + (n_\gamma^{\text{TAG}} > 0) + X(\text{missing})\}.$$

We consider here the  $B - L$  conserving decay modes:  $\tau^- \rightarrow \bar{\Lambda}\pi^-$  with  $\bar{\Lambda} \rightarrow \bar{p}\pi^+$  and  $\tau^+ \rightarrow \Lambda\pi^+$  with  $\Lambda \rightarrow p\pi^-$ . We also consider the  $B - L$  violating decay modes:  $\tau^- \rightarrow \Lambda\pi^-$  with  $\Lambda \rightarrow p\pi^-$  and  $\tau^+ \rightarrow \bar{\Lambda}\pi^+$  with  $\bar{\Lambda} \rightarrow \bar{p}\pi^+$ . The experimental signature for these modes is:

$$\{\tau^- \rightarrow (p\pi^-) + \pi^-\} + \{\tau^+ \rightarrow (\text{a track})^+ + (n_\gamma^{\text{TAG}} > 0) + X(\text{missing})\}.$$

We denote the pion from  $\tau \rightarrow \Lambda\pi$  as  $\pi_1$  and the pion from  $\Lambda \rightarrow p\pi$  as  $\pi_2$ . We can distinguish between the  $B - L$  conserving and violating modes by the charge of these pions: the  $B - L$  conserving decay modes have an opposite sign combination on the  $\pi_1$  and  $\pi_2$  charges, while the  $B - L$  violating modes have a same sign combination. As in the case of  $\tau^- \rightarrow \bar{p}\gamma$  and  $\bar{p}\pi^0$  modes, tracks and photons should have  $p_t > 0.1 \text{ GeV}/c$  and  $E_\gamma > 0.1 \text{ GeV}$ , respectively, with a polar angle satisfying  $-0.866 < \cos \theta < 0.956$ .

We first demand that the four tracks have a net zero charge. The magnitude of the thrust is required to be larger than 0.9 to suppress the  $q\bar{q}$  continuum background. The event should have a 1-3 prong configuration relative to the plane perpendicular to the thrust axis. We select  $\bar{\Lambda}$  candidates via the  $\bar{p}\pi^+$  decay channel based on the angular difference between the  $\bar{\Lambda}$  flight direction and the direction pointing from the interaction point to the decay vertex (see, Ref.[10] for more details). The proton from the  $\bar{\Lambda}$  decay is identified by demanding  $\mathcal{P}(\bar{p}/\pi) > 0.6$ . In order to avoid fake  $\bar{\Lambda}$  candidates in which two tracks in the signal side are an  $e^-e^+$  pair from a photon conversion, the electron veto is imposed on the three tracks in the signal side. The reconstructed  $\bar{\Lambda}$  candidate mass should be within  $\pm 5 \text{ MeV}/c^2$  of the nominal  $\Lambda$  mass and  $p_\Lambda^{\text{CM}} > 1.75 \text{ GeV}/c$  is required to reduce contributions from the generic  $\tau^+\tau^-$  and  $q\bar{q}$  continuum as shown in Fig. 4.

As in the  $\bar{p}\gamma$  and  $\bar{p}\pi^0$  cases, the following criteria are imposed:  $5.29 < E_{\text{vis}}^{\text{CM}} < 10.5 \text{ GeV}$  to reject Bhabha, two-photon and  $\mu^+\mu^-$  reactions;  $p_{\text{miss}} > 0.4 \text{ GeV}/c$  and  $-0.866 < \cos \theta_{\text{miss}} <$

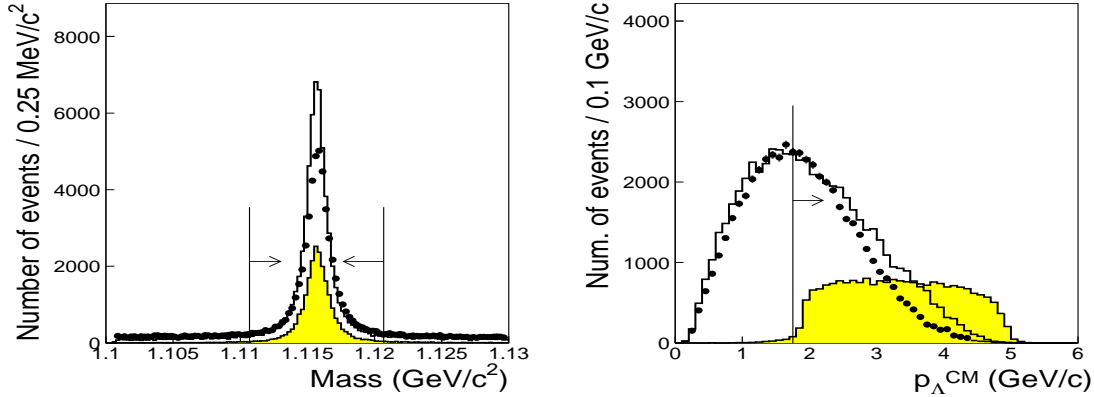


FIG. 4: Reconstructed  $\bar{\Lambda}$  candidate mass (left) and momentum (right) in the CM frame. The signal MC distributions are indicated by the filled histogram, all BG's including  $\tau^+\tau^-$  and  $q\bar{q}$  by the open histogram, and closed circles are data. While the signal MC is normalized arbitrarily, the data and MC are normalized to the same luminosity. The selected area is indicated by the lines with arrows.

0.956 to ensure that a missing particle is a neutrino(s);  $\cos\theta_{\text{miss-tag}}^{\text{CM}} > 0$  to include the missing particle in the tag side;  $n_{\gamma}^{\text{SIG}} \leq 1$  and  $n_{\gamma}^{\text{TAG}} \leq 2$  to suppress the continuum background.

Both the proton veto  $\mathcal{P}(\bar{p}/\pi) < 0.6$  and kaon veto  $\mathcal{P}(K/\pi) < 0.6$  are applied to  $\pi_1$  and the tag-side track.

The correlation between the missing momentum  $p_{\text{miss}}$  and mass-squared  $m_{\text{miss}}^2$  is considered to further suppress BG's from generic  $\tau^+\tau^-$  and continuum BG:  $p_{\text{miss}} > 1.5 \times m_{\text{miss}}^2 - 1.0$ .

### Signal resolutions and blind analysis

The  $M_{\text{inv}}$  and  $\Delta E$  resolutions are evaluated from MC:  $\sigma_{M_{\text{inv}}}^{\text{high/low}} = 4.6/4.0 \text{ MeV}/c^2$  and  $\sigma_{\Delta E}^{\text{high/low}} = 22/29 \text{ MeV}$ . In  $\bar{\Lambda}\pi^-$  ( $\Lambda\pi^-$ ), there is no  $M_{\text{inv}}$  tail due to energy leakage from ECL because there are no photons in the final state of this mode.

We blind a region over  $\pm 5\sigma_{M_{\text{inv}}}$  and  $-0.5 < \Delta E < 0.5 \text{ GeV}$ . Fig. 5 shows scatter-plots for data and MC samples over  $\pm 15\sigma$  in the  $M_{\text{inv}} - \Delta E$  plane: the number of data and MC events outside the blinded region (bounded by the vertical dotted line in Fig.5 (a) and (b)) are 11 and  $13.2 \pm 3.5$  events, respectively. Good agreement is observed. The surviving BG events are due to generic  $\tau^+\tau^-$  decays (about 1/2) and  $uds$  continuum (about 1/2). The former events are dominated by the  $\tau \rightarrow a_1(1260)\nu_{\tau}$  decays, in which three charged pions from the  $a_1(1260)$  decay form a fake  $\Lambda$  candidate. The continuum BG events have one true  $\Lambda$  which forms a signal candidate together with another track.

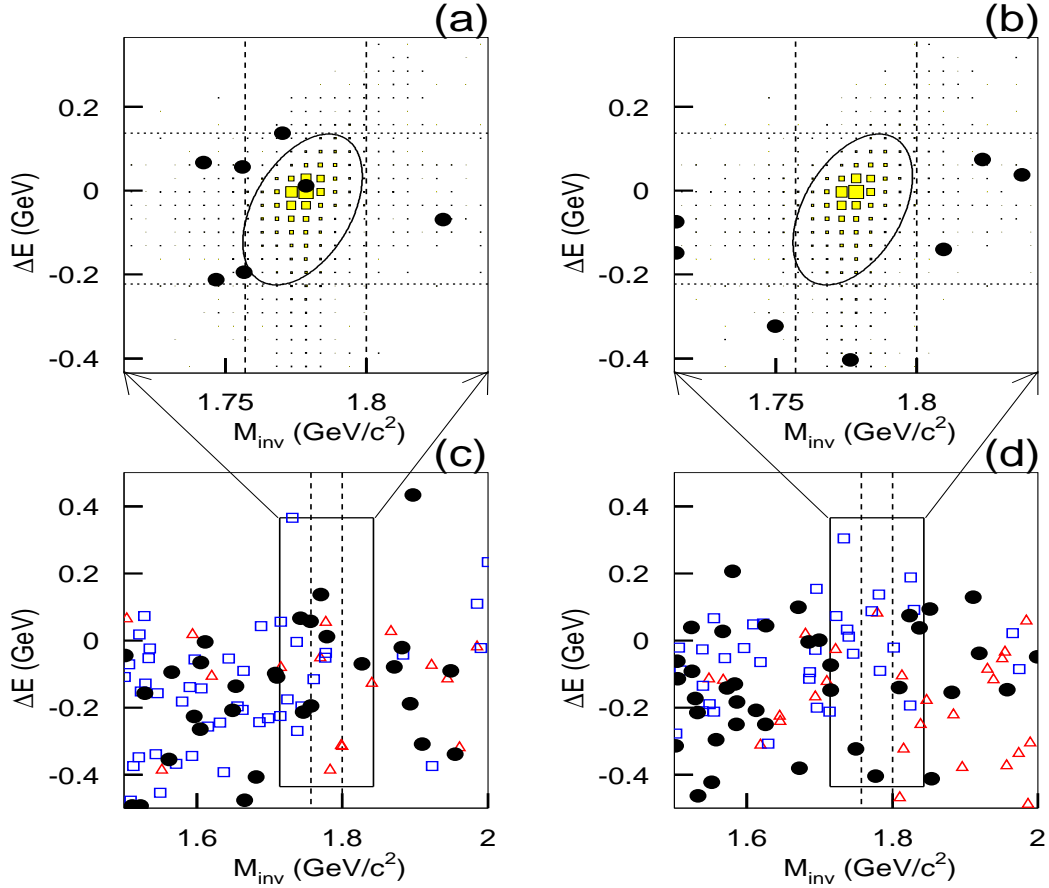


FIG. 5: Scatter-plot of data and MC events in the  $M_{\text{inv}} - \Delta E$  plane: (a) and (b) correspond to the  $\pm 15\sigma$  area for the  $B - L$  conserving and violating modes, respectively, while (c) and (d) show the region  $1.5 < M_{\text{inv}} < 2.0 \text{ GeV}/c^2$  and  $|\Delta E| < 0.5 \text{ GeV}$  for the same modes. The areas of (a) and (b) are also shown as solid rectangles in (c) and (d). The areas inside the dotted lines in (c) and (d) denote the blind signal regions. The 90% elliptical region shown by a solid curve in (a) and (b) is used for evaluating the signal yield. In (a) and (b) the vertical dotted lines denote the blind regions similar to those in (c) and (d); the regions inside the horizontal dotted lines and outside the vertical dotted lines are sidebands used to estimate the expected BG in the elliptical region. Closed circles correspond to the data ( $154 \text{ fb}^{-1}$ ), open squares are generic MC  $\tau^+\tau^-$  events (equivalent luminosity of  $297 \text{ fb}^{-1}$ ) and open triangles are MC  $uds$  continuum events (equivalent luminosity of  $104 \text{ fb}^{-1}$ ). Filled boxes show the MC signal distribution with arbitrary normalization.

## Blind opening and evaluation of the branching fraction

Since there are fewer remaining events compared to  $\bar{p}\gamma$  and  $\bar{p}\pi^0$ , we apply the Frequentist approach using the Feldman & Cousins method [11] rather than the maximum likelihood method. We take an elliptical region that contains 90% of MC signal events passing all cuts as a signal region, as shown in Fig. 5 (a) and (b). It results in the signal detection efficiency  $\varepsilon = 11.8\%$  for the  $B-L$  conserving and  $\varepsilon = 11.7\%$  for the  $B-L$  violating modes, respectively.

From Fig. 5 (c) and (d) we assume the BG distribution to be flat along the  $M_{\text{inv}}$  axis, and then obtain the expected BG in the ellipse as  $1.7 \pm 0.8$  events for each of the two modes, using sideband regions, inside the horizontal dotted lines and outside the vertical dotted lines, as shown in the Fig. 5 (a) and (b). We open the blinded region and find only one data event in the ellipse for the  $B-L$  conserving mode and no data events for the  $B-L$  violating mode (see Fig. 5 (a) and (b), respectively). The upper limits on the signal yields at 90% C.L. are obtained by the Feldman-Cousins method as  $s_{90} = 2.8$  and  $s_{90} = 1.2$ , respectively. The upper limits on the branching fraction are then calculated as

$$\mathcal{B}(\tau \rightarrow \Lambda\pi) < \frac{s_{90}}{2\varepsilon N_{\tau\tau} \mathcal{B}(\Lambda \rightarrow p\pi)} \quad (6)$$

where  $N_{\tau\tau} = 140.0 \times 10^6$  and  $\mathcal{B}(\Lambda \rightarrow p\pi) = 0.639$  [12]. The resulting values are  $\mathcal{B}(\tau^- \rightarrow \bar{\Lambda}\pi^-) < 1.3 \times 10^{-7}$  and  $\mathcal{B}(\tau^- \rightarrow \Lambda\pi^-) < 0.58 \times 10^{-7}$ .

Among systematic uncertainties on the detection sensitivity  $S_0 = 2\varepsilon N_{\tau\tau} \mathcal{B}(\Lambda \rightarrow p\pi)$ ,  $\bar{\Lambda}$  selection and the proton identification in  $\bar{\Lambda}$  decay contribute 6.0% and 3.0%, respectively;  $\mathcal{B}(\Lambda \rightarrow p\pi)$  has an uncertainty of 0.8% [12]; the trigger efficiency (0.5%), tracking (4.2%), selection criteria (4.0%), MC statistics (0.7%), luminosity (1.4%) and the  $\tau^+\tau^-$  cross-section (0.03%) are also considered. All these uncertainties are added in quadrature to 9.1% in total.

The upper limits on the branching fractions at the 90% C.L. including systematic errors are then calculated by the POLE program [13]. The resulting branching fractions are

$$\begin{aligned} \mathcal{B}(\tau^- \rightarrow \bar{\Lambda}\pi^-) &< 1.3 \times 10^{-7} \\ \mathcal{B}(\tau^- \rightarrow \Lambda\pi^-) &< 0.70 \times 10^{-7} \end{aligned}$$

at the 90% C.L.

## RESULTS

We obtain the following preliminary upper limits on the branching fractions:  $\mathcal{B}(\tau^- \rightarrow \bar{p}\gamma) < 3.0 \times 10^{-7}$ ,  $\mathcal{B}(\tau^- \rightarrow \bar{p}\pi^0) < 6.5 \times 10^{-7}$ ,  $\mathcal{B}(\tau^- \rightarrow \bar{\Lambda}\pi^-) < 1.3 \times 10^{-7}$  and  $\mathcal{B}(\tau^- \rightarrow \Lambda\pi^-) < 0.70 \times 10^{-7}$  at the 90% confidence level.

For the latter two modes this is the first search ever performed.

The resulting upper limits on the branching fraction for  $\tau^- \rightarrow \bar{p}\gamma$  and  $\tau^- \rightarrow \bar{p}\pi^0$  improve upon the previous measurements by a factor of 12 and 23, respectively. This large improvement is mostly due to the powerful proton identification ability of the Belle detector that removes spurious combinatorial BG's as well as higher statistics compared to the previous experiment.

### Acknowledgments

We thank the KEKB group for the excellent operation of the accelerator, the KEK Cryogenics group for the efficient operation of the solenoid, and the KEK computer group and the National Institute of Informatics for valuable computing and Super-SINET network support. We acknowledge support from the Ministry of Education, Culture, Sports, Science, and Technology of Japan and the Japan Society for the Promotion of Science; the Australian Research Council and the Australian Department of Education, Science and Training; the National Science Foundation of China under contract No.10175071; the Department of Science and Technology of India; the BK21 program of the Ministry of Education of Korea and the CHEP SRC program of the Korea Science and Engineering Foundation; the Polish State Committee for Scientific Research under contract No. 2P03B 01324; the Ministry of Science and Technology of the Russian Federation; the Ministry of Education, Science and Sport of the Republic of Slovenia; the National Science Council and the Ministry of Education of Taiwan; and the U.S. Department of Energy.

---

\* on leave from Nova Gorica Polytechnic, Nova Gorica

- [1] For example, G. Lazarides, C. Panagiotakopoulos and Q. Shafi, Nucl. Phys. B **278**, 657 (1986).
- [2] W. S. Hou, M. Nagashima and A. Soddu, arXiv:hep-ph/0404002.
- [3] S. Kurokawa and E. Kikutani, Nucl. Instr. Meth. A **499**, 1 (2003), and other papers included in this Volume.
- [4] R. Godang *et al.* (CLEO Collaboration), Phys. Rev. D **59**, 091303 (1999).
- [5] A. Abashian *et al.* (Belle Collaboration), Nucl. Instr. and Meth. A **479**, 117 (2002).
- [6] KORALB/TAUOLA: S. Jadach and Z. Was, Comp. Phys. Commun. **85**, 453 (1995).
- [7] QQ - The CLEO Event Generator (<http://www.lns.cornell.edu/public/CLEO/soft/qq/>).
- [8] R. Brun *et al.*, GEANT 3.21 CERN Report No. DD/EE/84-1, 453.
- [9] I. Narsky, Nucl. Instr. and Meth. A **450**, 444 (2000).
- [10] K. Abe *et al.* (Belle Collaboration), Phys. Rev. D **65**, 091103 (2002).
- [11] G.J. Feldman and R.D. Cousins, Phys. Rev. D **57**, 3873 (1998).
- [12] S. Eidelman *et al.* (Particle Data Group), Phys. Lett. B **592**, 1 (2004).
- [13] J. Conrad *et al.*, Phys. Rev. D **67**, 012002 (2003).